Chapter Three

The Generation and Nature of X-rays

3. Introduction

We have come to regard x-rays as an important component of electromagnetic radiation. Today, x-rays are used in a wide variety of applications ranging from sophisticated high-energy-physics and astrophysical projects, to the routine examination of "carry-on luggage" in all airports. In all applications, the x-rays are generated by the bombardment of matter with high-energy particles, usually electrons. For the purposes of this course it is necessary to have a relatively good understanding of x-rays -- not only in terms of how they are generated, but also in terms of how they interact with their surrounding atoms, and how they can be detected and utilized for informational purposes.

3.1 A Brief History

The term *x-ray* was first proposed in 1885 by its discoverer, Wilhelm Roentgen, Professor of physics in Würzburg, Germany. In the course of his research, Roentgen noticed effects of "invisible radiation" while experimenting with electron beams produced by recently developed cathode ray tubes. The effects he noted included the production of short-wavelength and visible radiation that could be observed on exposure of photographic emulsions. The properties of the invisible (short-wavelength) radiation also included high degrees of transparency through all materials, and straight-line trajectories that are uninfluenced by magnetic fields.

Subsequent research by Winkelmann and Straubel discovered *fluorescence* of secondary x-rays by "primary" x-rays. Haga and Wind discovered the diffraction of x-rays by solid materials, and concluded that the wavelength of such radiation must be on the order of 10^{-10} meters. Laue demonstrated with the dispersion of x-rays that their wavelength must be on the order of atomic dimensions. Subsequently, the wavelengths of characteristic x-ray radiation were measured to be in the range of 10^{-8} to 10^{-11} meters, and the dimensional unit angstrom ($Å=10^{-10}$ m) was introduced.[1]

---

[1]   Although not recognized today as a international unit, the angstrom is still used when referring to inner-atomic distances and x-ray wavelengths.

The theory of diffraction of x-rays, originally proposed by Laue, was conclusively demonstrated by W.H. Bragg and W.L. Bragg in 1913 by obtaining the first x-ray diffraction pattern a sodium chloride crystal (for which they won the Nobel Prize).

Meanwhile, H.G.J. Moseley (1913) was researching the characteristics of x-ray emission from different target materials. He noticed a systematic progression of x-ray wavelengths with increasing atomic number of the material generating the radiation. Based on this regularity, the previously unknown elements hafnium and rhodium were discovered with x-ray spectral analysis.

As is common in science, the experimental observation of important phenomena occurred before it could be explained fully by theory. Max Planck in 1900 first began to analyze atomic structure in terms of the then-developing **quantum theory** of energy. Planck proposed that an oscillating (ionized) atom could not have any arbitrary energy, but rather only certain selected energy values (quanta) were possible. Planck reasoned that if only certain energy levels were possible, there ought to be a relationship between the energy of an atom undergoing change and both the energy and wavelength of the radiation emitted during the process. He suggested that the wavelength of electromagnetic radiation, λ, its frequency, ν, and its energy, E, are related:

$$E = nh\nu = \frac{nhc}{\lambda}$$

(electron volts) eq. 3-1

where n is a positive integer, h is Plank's constant (6.626×10^{-34} Joule·sec), and c is the speed of light (3.0×10^{8} meter/sec). In x-ray physics, E is measured in *electron volts*, eV, and is a unit of energy (1.6021×10^{-19} J/eV), such that

$$E\lambda = hc = 12{,}397$$

(eV·Å) eq. 3-2

An often asked question is the difference between volts and electron volts. They are often equated, i.e., if an electron is exposed to a potential of 10kV, it is said to have 10keV worth of energy. But strictly speaking, the volt is a unit of potential energy, and is not related to kinetic energy (or work), unless a charged particle (e.g., an electron with charge e, the elementary charge) is accelerated by a potential difference.

The first application of the quantum theory of atomic structure was made in 1913 by Niels Bohr (the same year in which the Braggs published their paper on x-ray diffraction). Bohr developed a model of the hydrogen atom, which allowed him to explain why the observed frequencies (i.e., wavelengths) of energy emitted obeyed simple relationships. Although it was later shown to be too simplistic, Bohr's model allowed him to calculate the energies of the allowed states for the hydrogen atom. Subsequent refinements in the theory of atoms by Heisenberg, De Broglie and Schrödinger have resulted in our modern view of quantum mechanics. For our purposes, quantum mechanics are important to the extent that they describe the transitions that are possible during the interaction of highly energetic, beam electrons and electrons within target atoms with great accuracy. The principle quantum numbers are summarized below:

CHAPTER THREE

THE GENERATION AND NATURE OF X-RAYS

1. ***The principle quantum number (n)***: The principle quantum number (n) can include any positive integral value. It determines the major energy level of an electron. It is designated **K**, **L** and **M** for n = 1, 2 and 3 respectively. The maximum number of electrons allowed is $2n^2$.

2. ***The azimuthal momentum quantum number (l)***: The azimuthal or angular momentum number can be considered to represent sub-shells within the major energy levels. The sub-shells correspond to "orbitals". Higher values of *l* correspond to greater angular momentum (mvr). *l* may assume integer values from 0 to **n**-1. The orbitals are **s, p, d** and **f** for *l* = 0, 1, 2 and 3 respectively. The orbitals have distinctive shapes. The maximum number of electrons allowed is: **s** = 2, **p** = 6, **d** = 10 and **f** = 14.

3. ***The magnetic quantum number (m)***: An electron with angular momentum generates a magnetic field. **m** can assume any integer from -*l* to +*l*.

4. ***The spin quantum number***: A small "particle", like an electron, spinning on its own axis also behaves as a small magnet, hence the electron itself has an intrinsic magnetic property. We say that the electron has a **spin** and describe it as being either +1/2 or -1/2.

Summary for K, L and M Shells

n	*l*	Orbital	m	s	maximum # (e^-)
1	0	1s	0	+1/2, -1/2	2
2	0	2s	0	+1/2, -1/2	2
2	1	2p	-1, 0, +1	+1/2, -1/2	6
3	0	3s	0	+1/2, -1/2	2
3	1	3p	-1, 0, +1	+1/2, -1/2	6
3	2	3d	-2,-1,0,+1,+2	+1/2, -1/2	10

The specific quantum numbers assigned to the electrons are determined by thermodynamic considerations that require the occupation of states having the lowest energies first, and the Pauli Exclusion Principle, which forbids more than one electron in an atom to have the same four quantum numbers (by definition). In addition to considering the orbitals of an atom, it is, from an energetic point of view, necessary to take into account the influence that interactions between the magnetic moments of the spin and the orbital motion of an electron have on its energy. In order to describe the consequences of these spin-orbit interactions, it is convenient to define a new quantum number:

$$\mathbf{j} \equiv l \pm \mathbf{s}$$

In other words, "**j**" is the vector sum of *l* and **s.**

3-3

Shell	K	L			M				
n	1	2			3				
l	0	0	1		0	1		2	
j	1/2	1/2	1/2	3/2	1/2	1/2	3/2	3/2	5/2
E	K	L(I)	L(II)	L(III)	M(I)	M(II)	M(III)	M(IV)	M(V)

Notice that in this table the usual electronic picture of an atom is not changed. The importance of this table is that it shows different energy levels within each of the various orbitals. One can not only distinguish the **s** from the **p** electrons by their *l* value (*l*=0 for s, and *l*=1 for p), but one can also distinguish two kinds of **p** electrons depending on whether **j** is greater than, or less than *l*. Notice, for example, that there are three distinct energy levels for the L electrons (L$_I$, L$_{II}$, and L$_{III}$) and five different energy levels for the M electrons.

Atoms release energy when they undergo transitions from a higher energy state to a lower energy state. For example, if an electron moves from the L$_{III}$ energy level to the K state, a quantum of energy equal to (E_K - $E_{L(III)}$) is released. There are many possible transitions, dependent only on the availability of electrons in a particular shell (i.e., on the element's atomic number). Some of the transitions are, however, more probable than others, and some are in fact prohibited. The Pauli Exclusion Principle, when applied to energy transitions, predicts that some transitions are not possible, thus leading to a set of "selection rules". The rules that predict commonly observed transitions (and forbid others) are

$$\Delta n \ < \ 0, \quad \Delta l \ = \ \pm 1, \quad \Delta j = 0 \pm 1$$

The change in *n* allows only a direction of lower energy in integer amounts of quanta; a change in *l* must be either plus or minus 1, and a change in *j* must be -1, 0 or +1. Examination of the above table demonstrates, for example that the transition from L$_I$ to K does not occur because both of these electrons are **s** electrons and hence there is no change in *l* .

3.2 Generation of x-rays

Energy transitions in atoms can only occur if the atom is first perturbed by some "external" source of energy. Normally, atoms exist in their lowest energy, or ground state. If an atom is "excited" by an input of energy, it is thermodynamically unstable and will respond by electron transitions that result in a lowering of the atom's energy. For our purposes, excitation of atoms results from bombardment of the target (specimen) with high-energy electrons in the incident beam. The most energetic of transitions are those involving the K-shell electrons since they are the most tightly bound to the nucleus.

Figure 3-1 illustrates excitation of an atom by ejection of a K-shell electron by an inelastic collision with an electron from the beam. In order to excite an atom by ejecting a K-shell electron (to a distance outside the atom), the incident beam must have an energy greater than the energy required to remove a K-shell electron (E_K). **If** the incident beam has sufficient energy, and **if** an inelastic event occurs between an incident electron and a K-shell electron, then the K-shell electron can be ejected from the atom. The incident beam electron loses a quantum of energy equal to that required to eject the K-shell electron, and is scattered with little change in its trajectory.

The process of ejecting a K-shell electron creates an *electron hole* in the K shell and raises the energy level of the atom to the "K-state". This energy level is thermo-dynamically unstable and the atom will instantaneously respond by filling the electron hole with another electron from an outer orbital. The nearest electrons are in the L shell, and hence are the most probable electrons to fill the electron hole. The process of an electron moving from the L shell to the K shell is called the Kα transition. If the L electron is in the L_{III} energy state, the transition is called the **Kα₁** transition. Energetically, the filling of the electron hole by an L_{III} electron lowers the energy state of the atom by
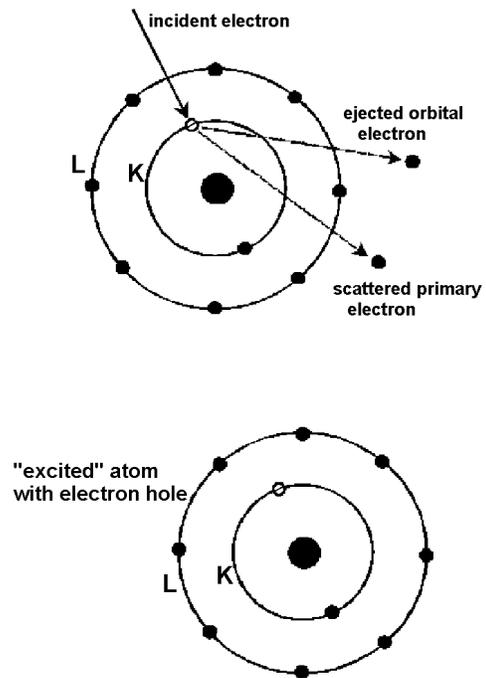

Figure 3-1   Schematic diagram illustrating the ejection of an K-shell electron and production of an unstable electron hole.

$$E_{(K\alpha 1)} \; = \; E_K \; - \; E_{L(III)}$$
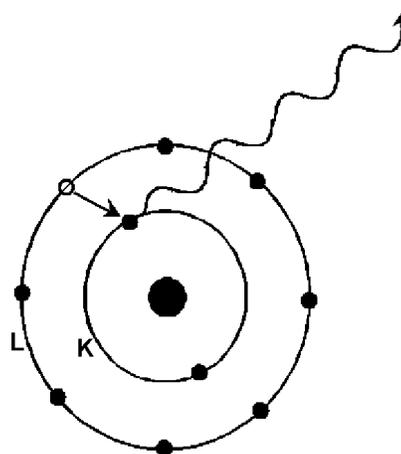
3.2.1 Characteristic x-rays

Owing to the fact that energy can neither be created nor destroyed, the energy change for this process must be released in some other form. The energy released is given off in the form of an x-ray photon with energy equivalent to the above energy balance. Equations 3-1 and 3-2 show that the wavelength of this photon will also be determined by the energy transition. Since the energy released in this transition is a fundamental property of the element, such x-rays are called *characteristic x-rays*.

electron hole is filled and x-ray photon generated

Figure 3-2   Schematic drawing illustrating the origin of a K-shell x-ray.

It is also possible that the vacancy can be filled by an L_{II} electron. This transition gives rise to the $K\alpha_2$ photon. The energy difference between the L_{II} and the L_{III} quantum states is very small, and hence the energy and wavelength of the $K\alpha_1$ and the $K\alpha_2$ are very similar. These two peaks therefore effectively form a doublet and are not usually resolvable by most instruments. Another possibility is that the K-shell electron hole is filled by an electron from the M-shell. This type of transition gives rise to the $K\beta$ series of x-ray lines. There are two permitted lines in this series: the $K\beta_1$ (K -M_{III}) and the $K\beta_3$ (K - M_{II}). The minimum energy required to produce all K photons ($K\alpha$ and $K\beta$) is called the *critical excitation energy*, $K_{C,K}$.

If an $L \Rightarrow K$ transition occurs, an electron moves from L to K filling the hole in K, but at the same time creating a hole in L. This vacancy can be filled by electrons from the M-shell, giving rise to the *L-series* of x-ray lines. The same thing happens, of course, if an incident beam electron ejects an L electron to start with. *As long as an atom contains electrons in the various outer shells, if the K-series is excited, then the L and M series will also be excited!*

3.2.2 Moseley's law.

The practice of x-ray analysis and the modern study of x-ray physics rely on *Moseley's Law* with regard to the predictability of x-ray energies as a function of atomic number. Historically however, Moseley's Law deals with the energy needed to generate an x-ray; that is, the amount needed to remove the electron from the inner atomic shell, E_q, which is related to the minimum potential, V_q, required to eject the electron with an electronic charge, *e*.

Moseley's law is a function of atomic number, Z,

$$E_q = eV_q \propto (Z\sigma)^2$$

eq. 3-3

where the proportionality and the "screening constant", σ, differ depending on which inner shell (K, L, etc.) is ionized. To a first approximation, the relationship also holds for the energy of the resultant x-rays because the critical energy required for shell ionization is only slightly greater.

Figure 3-3 shows very clearly how the families of lines disperse with increasing atomic number. That is, with increasing atomic number or energy, the lines within a particular family spread themselves across an increasing range of energy. In the case for lighter elements, most instruments can not resolve $K\alpha_1$ and $K\alpha_2$. They are distinct transitions, but not separable, and are commonly notated as $K\alpha_{1,2}$ or just $K\alpha$. In reference tables which list all detectable

Figure 3-3   Moseley's Law for several x-ray lines and absorption edges (from Heinrich, 1981).

lines from all known sources, these unresolvable lines pairs, or doublets, will be listed separately, but the weighted average location for both will also be listed, as if it were one line. Its relative intensity will also exceed the normalized value of 100; for example, in the above case where one line has an intensity of 100 and the other a relative value of 50, the combined value will be 150. Do not read these intensity values in an absolute or accurate sense, as they are only meant to be a rough guide and only in regard to that specific element. Also the relative intensities from one family (for example, K series) should not be compared to the relative intensities from another family. In absolute intensity, the L series tend to be much less intense than the L series and the M series even less intense. This is partially due to the probability of a particular shell being excited in an atom with many shells.

Figure 3-4 illustrates the energy level diagram for gold. Even with the prohibited transitions removed, there are clearly a large number of transitions and distinct x-rays produced. As a guide to reading such a diagram, note that the energy for the gold $K\beta$ transition and its subsequent x-ray is the difference between the two shells, 8×10^4 minus 3×10^3 or 77keV (the scale is logarithmic), and for a lower energy transition, e.g., $L\beta_2$, the energy would be approximately 1.2×10^4 minus 4×10^2 or 11.6keV.
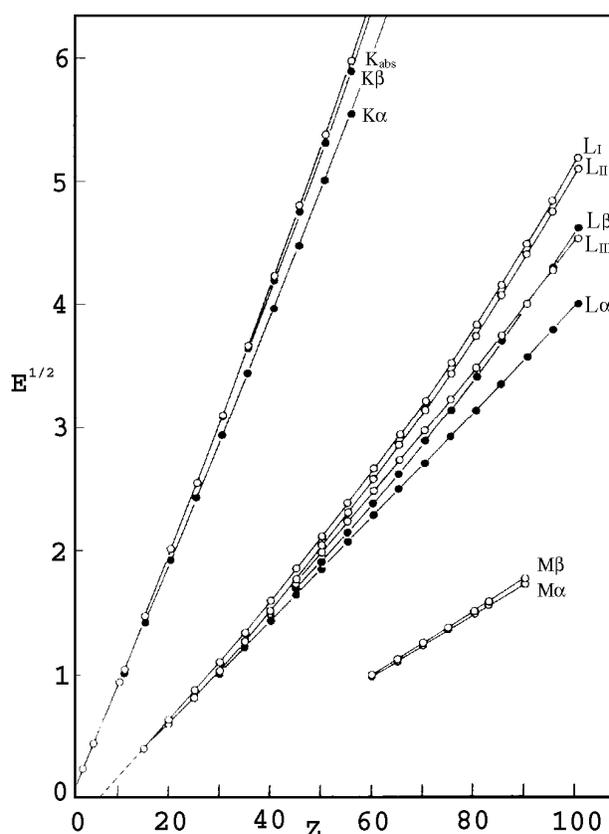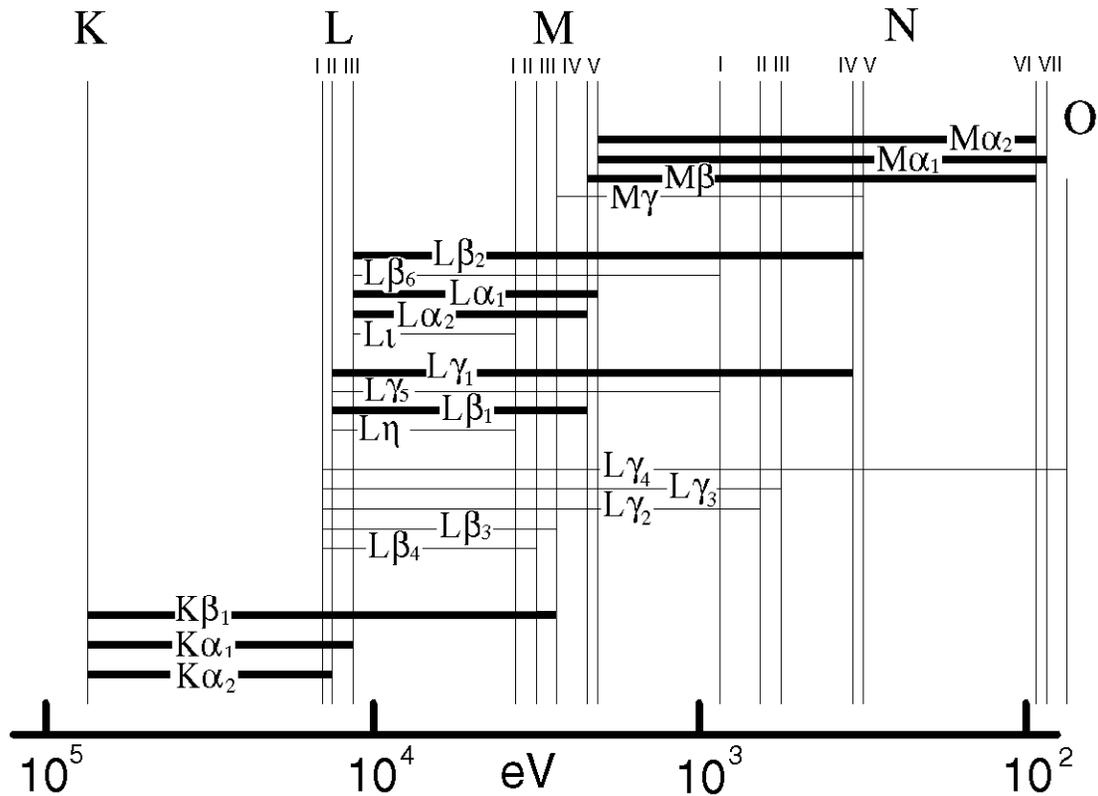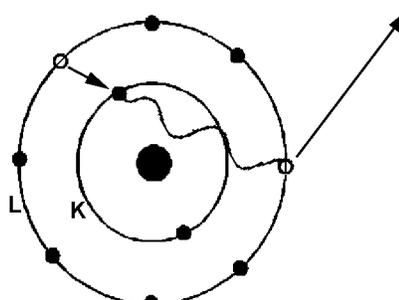
Figure 3-4 The atomic energy level diagram for gold. Lines commonly used for EPMA are weighted bold, and the lines that are forbidden are not shown (from Heinrich, 1981).

Inner shell ionizations can happen by way of two different mechanisms within a target being bombarded with energetic electrons. *Primary* ionization occurs when an inner shell is ionized by a primary electron, and *secondary* ionization can occur if the inner shell electron is ejected by the way of interaction with an x-ray emitted from another atom x-ray. The latter mechanism, more commonly referred to as *fluorescence*, can only happen if the incoming x-ray is of high enough energy. For example, an Fe Kα x-ray (6.403keV), or even the more energetic Fe Kβ (7.057keV) cannot ionize an Fe K shell (E_c=7.110keV) because the x-ray is always of lower energy than the corresponding ionization energy for that respective shell. Referring to Figure 3-3, the critical ionization energy, E_c, required for each shell is read directly off the energy axis, i.e., zero energy on that axis refers to an electron "far removed" from the atom's influence. An example of Fe Kα (E_c=7.110keV) fluorescence would occur in the presence of nickel radiation ($Ni_{K\alpha}$=7.477keV), e.g., in alloys of steel.

3.2.3   Fluorescence yield

For each inner-shell ionization, there are two possible outcomes: 1) the photon generated by the transition escapes from the atom in the form of a characteristic x-ray; or 2) the x-ray photon is internally consumed by interaction with outer-shell electrons.   The latter possibility is illustrated in Figure 3-5. Since the energy of the K photon is greater that the critical excitation energy for an L-shell electron, the photon may eject an L-shell electron. The energy of the K photon is converted into the energy necessary for L-ionization plus the kinetic energy of the new ejected electron. Such electrons are called Augér electrons after P. Augér who first discovered them in 1925. (Pronounced "O-jshay")

The *fluorescent yield,* ω, is the probability that an x-ray will be emitted as a result of ionization of a specific shell. For a given series of x-ray lines (e.g., the K series), ω is numerically equal to the ratio of K photons escaping from the atom to the ratio of original K-shell ionizations. Since the only other possibility is production of an augér electron, the sum of the yields of x-ray photons and Augér electrons from a given atom will be unity (1.0).   The fluorescent yield for K lines increases monotonically as a function of atomic number, and algebraic models accurately predict the empirical data. The fluorescent yield increases with atomic number.   As examples zinc (Z=30) has $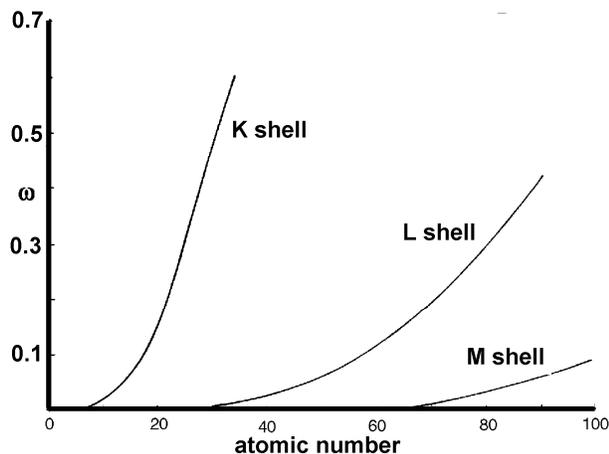\omega_K$ = 0.45, but sodium (Z=11) is only 0.02.   In other words, of all the K photons produced in sodium, only 2% are able to escape from the atom. This factor means that the sensitivity of the x-ray method decreases for the lighter elements.   The decrease, however, is partly compensated by the fact that x-ray production in low-Z elements is increased owing to the relatively low critical energies required for K-shell ionizations.

x-ray photon is internally consumed and Auger electron emitted

Figure 3-5 Schematic diagram illustrating the internal consumption of an x-ray photon and production of a Augér electron.

Figure 3-6   Fluorescence yield, ω, for the K, L and M families of x-rays as a function of atomic number (Goldstein et al., 1984).

Table 2.   X-ray Lines and Transitions[2] (Bertin, 1971)

	Initial Ionization Level								
Transition level	K	L_I	L_{II}	L_{III}	M_I	M_{II}	M_{III}	M_{IV}	M_V
L_I									
L_{II}	$K\alpha_2$								
L_{III}	$K\alpha_1$								
M_I			$L\eta$	$L\iota$					
M_{II}	$K\beta_3$	$L\beta_4$		$L\sigma$					
M_{III}	$K\beta_1$	$L\beta_3$	$L\beta_{17}$	$L\tau$					
M_{IV}	$K\beta_5$	$L\beta_{10}$	$L\beta_1$	$L\alpha_2$					
M_V	$K\beta_5$	$L\beta_9$		$L\alpha_1$					
N_I			$L\gamma_5$	$L\beta_6$					
N_{II}	$K\beta_2$	$L\gamma_2$						$M\zeta_2$	
N_{III}	$K\beta_2$	$L\gamma_3$							$M\zeta_1$
N_{IV}	$K\beta_4$		$L\gamma_1$	$L\beta_{15}$			$M\gamma_2$		
N_V	$K\beta_4$			$L\beta_2$			$M\gamma_1$		
N_{VI}			$L\upsilon$					$M\beta_1$	$M\alpha_2$
N_{VII}			$L\upsilon$						$M\alpha_1$
O_I			$L\gamma_8$	$L\beta_7$					
O_{II}		$L\gamma_4$							
O_{III}	$K\delta_2$	$L\gamma_4$							
O_{IV}	$K\delta_1$		$L\gamma_6$	$L\beta_5$					
O_V				$L\beta_5$					

---

[2]   Boxed transitions are x-ray lines commonly used for electron probe microanalysis. The shaded areas indicate violation of the principal quantum number rule, and are strictly forbidden. Where two transitions cannot be resolved (e.g., $K\alpha_1$ and $K\alpha_2$), both transitions are given the same nomenclature (e.g., $K\alpha$).

When we correct raw intensity data from the microprobe to determine weight fractions of the elements present, we depend on understanding factors like the fluorescent yield. When you choose to measure an element with its much lower energy L line rather than its K line, you exploit what we have been able to model accurately using our knowledge of physics. On the other hand, if you choose a standard that is close in composition to the unknown, then this kind of complication is likely to affect both the standard and unknown equally, and contribute little to the final analysis.

The fact that characteristic x-ray photons are described by either their energy or their wavelength enables us to isolate and count x-rays for a desired element either by discrimination baseed on energy or by wavelength. This fact produces two principal types of x-ray detection systems:

WDS: wavelength dispersive detection system in which x-rays from different elements are recognized and separated from one another by their wavelength using Bragg diffraction.

EDS: energy dispersive detection system in which x-rays from different elements are recognized and separated from one another by their characteristic energy using a solid state detector and multichannel analyzer.

Some Examples:

		Wavelength (λ)			**Energy (keV)**	
Z	**Name**	**Kα_1**	**Kα_2**	**Kβ_2**	**Kα**	**Kβ**
11	Na	11.909	11.909	11.617	1.041	1.041
14	Si	7.125	7.128	6.768	1.739	1.838
26	Fe	1.936	1.940	1.757	6.398	7.057
92	U	0.126	0.131	0.109	97.143	111.786

3.2.4 X-ray line intensities

Modern x-ray detection systems are not only capable of measuring or separating the x-rays from one another by either wavelength or energy, but are also capable of measuring the *intensity (I)* of the characteristic x-rays as well. Intensities are usually measured as a rate (e.g., the number of x-ray photons detected per second) or as the total number of x-ray photons detected in a given time period (e.g., number of photons in 10 seconds counting time). These intensities are also usually normalized to the electron beam current for quantitative purposes since the number of x-ray produced is exactly proportional to the number of electron hitting the sample. Corrections for detector counting losses (deadtime), background and drift will be discussed later on.

The relative intensities of lines depend, to a first approximation, on 1) the number of electrons available; 2) the selection rules; and 3) the probability of the energy transition producing

a given photon. When a given line in a series is present for an element, all of the permitted lines in that series is also present. This means that the critical excitation energy for that elemental series has been exceeded by the electron beam.

Of prime importance for quantitative analysis is the fact that, at least to a first approximation, the intensity of a given x-ray line is proportional to the concentration of the element emitting that line in the sample (strictly speaking the number of atoms present). We can then say that the intensity of x-radiation produced by an element i is proportional to the concentration of i in the sample. For two specimens bombarded under identical conditions (i.e., identical beam voltage and current):

$$\frac{C_i^1}{C_i^2} = \frac{I_i^1}{I_i^2}$$

<div align="right">eq. 3-4</div>

If one of the specimens is a ***"standard"*** in which the concentration of element i is precisely known, the above equation can be used to obtain a semi-quantitative analysis of i in the other (unknown) specimen. As we will see, however, this is just an approximation — there are many factors that affect the intensity of x-radiation other than just concentration of the emitting element.

From the sort of considerations we have just discussed, you might believe that a typical x-ray spectrum might appear as in the example in figure 3-7. In this ideal example, the individual vertical lines correspond to x-ray lines from different elements in a multi-element specimen, in this case the example might be olivine. The height of the lines is a measure of the x-ray emission intensity, and ideally, the height should be a measure of the weight percent of that element. In reality, typical x-ray spectra appear quite different. First of all, the x-ray lines are really "peaks" and in some cases can be quite broad. Peak broadening can result from (1) x-ray lines overlapping (e.g., $K\alpha_1$ and $K\alpha_2$), (2) features related to the local atomic environment (see below), and from

Figure 3-7 Hypothetical, ideal x-ray spectrum from a multi-element specimen, (e.g., olivine).

resolution limits of the x-ray detection system. In addition, the above "ideal" example shows the x-ray lines to rise from a zero baseline. In other words, it shows a spectrum with no background "noise". In reality however, background noise does need to be measured and removed. Furthermore, x-ray intensity is not an absolute measure of the element's concentration, and inefficiencies for x-ray generation and measurement need to be considered.
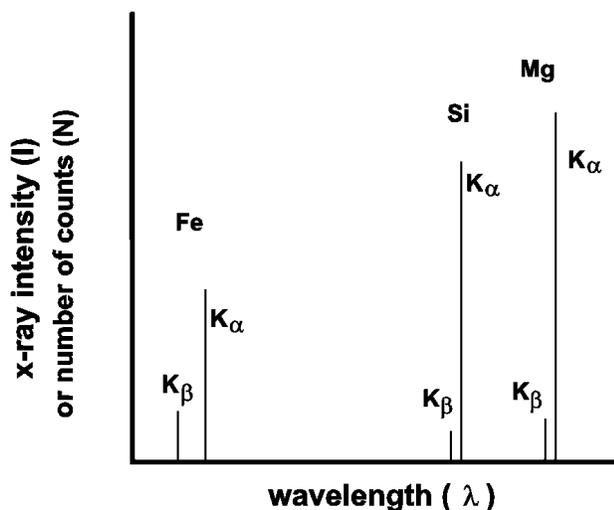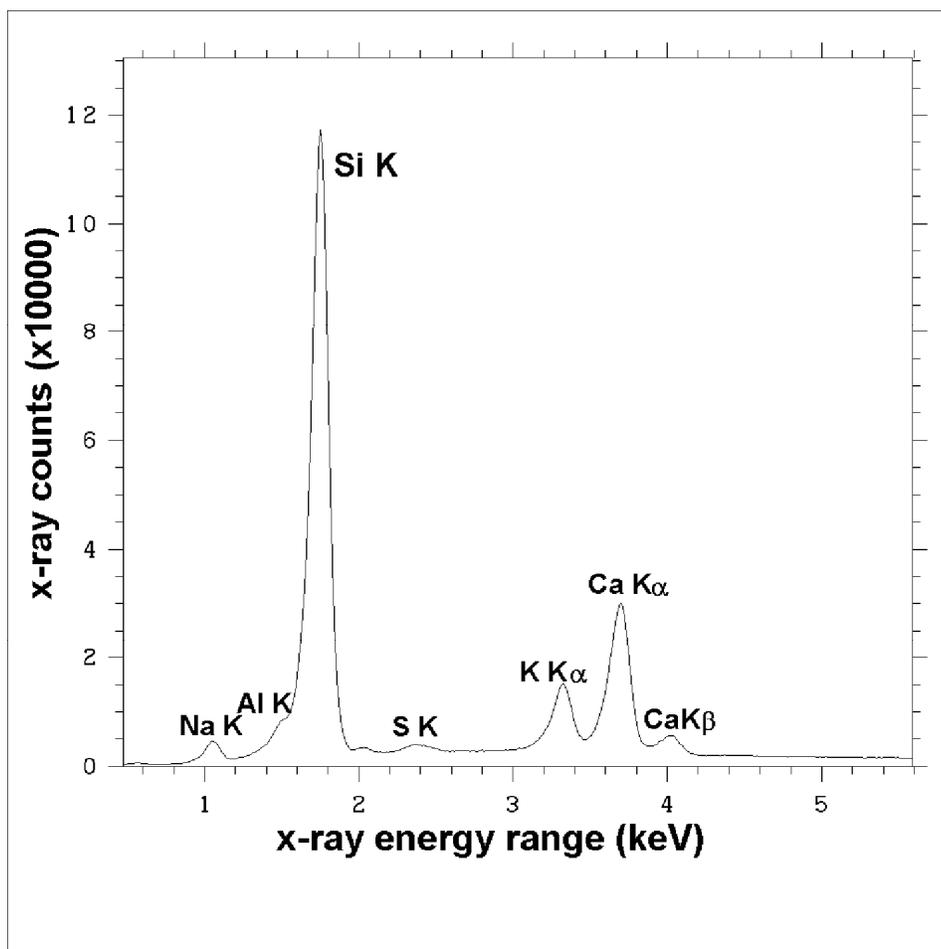
Figure 3-8   EDS spectrum of a hydrothermal slag specimen.

Figure 3-8 shows a typical EDS x-ray spectrum for a silicate slag (hydrothermal ore) plotted against energy (instead of wavelength). The figure clearly illustrates that the x-ray lines do not rise from a zero-baseline, but are superimposed upon a significant background. Furthermore, it is apparent that the background is not everywhere uniform, but has a definite shape to it. The background radiation is known (1) simply as the *background*, (2) *the continuous x-ray spectrum* or *continuum*, or (3) the by German term "*bremsstrahlung*". This background radiation results from energy released from primary beam electrons that are decelerated by the Coulombic field surrounding atoms within the specimen. The German term translates into "braking radiation" and accurately portrays the loss of kinetic energy suffered by incident electrons by the Coulomb fields associated with atoms. As incident electrons are slowed down, they release radiation. Since the degree of "braking" can, in principle, be continuous from zero to complete stoppage, the energy released in this process spans the range from zero to that of the primary beam energy. The intensity of the continuous radiation is, however, not constant over the entire energy (or wavelength) range, but exhibits a pronounced hump skewed toward lower energies. This is because the probability of a primary electron losing most or all of its energy in a single bremsstrahlung event is very small.

The existence of the continuum means that the number of x-ray photons counted (detected) when a spectrometer is "tuned" to a particular x-ray line is really the sum of the characteristic photons and the background counts ($I_{measured}$ = $I_{characteristic}$ + I_{bkg}). This implies that in order to obtain a true measure of the x-rays of interest we must subtract the background "counts" from those of the line of interest. This in turn means that for quantitative analysis we must not only measure the "peak" of interest, but also the background on either side of the peak. Furthermore, the detection and measurement of elements present in trace amounts requires that attention be given to the peak to background ratio (P/B).

An approximate expression for the intensity distribution of the continuum as a function of wavelength (λ) observed over a sample under electron beam excitation is given by:

$$I_{cont} \quad \propto \quad i_b Z (\lambda_o^{-1} - \lambda^{-1}) \lambda^{-1}$$

<div align="right">eq. 3-5</div>

for which i_b is the electron flux in the incident beam ("beam current"), Z is the mass average atomic number of the target (approximated by $Z = \Sigma_i C_i Z_i$ where C_i is the mass fraction of element i), and λ_o is the short wavelength limit of the continuum as determined by E_o:

$$\lambda_o = 12,398/E_o$$

From the above expressions, it can be seen that the background radiation is directly proportional to the beam current and to Z. This has some important implications. Lets say you are interested in analyzing a minor or trace element. Since this element is present in small amounts, it might appear that the obvious thing to do is to increase the beam current so as to increase the intensity of x-rays produced by that element. The problem is that as you increase the beam current, you also increase the background, and you may in fact not see an improvement in the peak/background ratio. Counting for longer periods of time may turn out to be a more practical solution though normally it is useful to increase the beam current to the maximum level at which the samples is not being damaged by the beam. Peak/background ratios become extremely important for trace elements and in defining the lower concentration limit at which elements can be measured within specified confidence limits. This is known as the *minimum detection limit* -- a subject we will discuss in more detail later.

3.2.5 X-ray Peak Shapes[3] and Positions

As noted above, x-ray peaks always have finite widths attributable to a combination of specimen and instrumental characteristics. Examination of the energies or wavelengths of the Kα_1

---

[3] The term "peak" refers to instrumental inability to measure absolute energies (or wavelength), and, indeed, there is a natural distribution about theoretical energies, such that we actually see a distribution about the theoretical energy. "Peak" then refers to the modal energy, and shape refers to the distribution.

and $K\alpha_2$ lines indicates that it would be virtually impossible to separate them with instruments of typical resolution.. Hence they effectively form a doublet of finite width. As atomic number increases, the energy separation between the $K\alpha$ and $K\beta$ x-rays increases, but for low-Z elements, these two may not be completely separable. The $K\beta$ peak may appear as a "shoulder on the high-energy side of the stronger $K\alpha$ peak. Furthermore, in low-Z elements (especially those in Period 2) the K-shell electrons may be influenced by nearest-neighbor atoms to which they are bonded.

When we speak of x-rays emitted, we always speak in terms of quantum-mechanical *transitions*, because it is the transition of an electron from a outer shell to an inner ionized shell that is responsible for a given x-ray peak. The x-rays which result from these inner shell ionizations are theoretically exact in terms of energy, and are said to be *characteristic*. In principle, therefore, x-ray line widths and peak shapes ought to be narrow and symmetrical. Examination of x-ray spectra, however, shows that high-energy, K peaks (i.e., K x-rays from high-Z elements) generally are relatively narrow and symmetrical, but those from very light elements (Z=16) are often broad, asymmetrical and "lumpy". A similar phenomenon is observed for the L peaks of very high-Z elements. Although this phenomenon is not completely understood, it is clear that part of the issue is that the energy of K-shell electrons in low-Z elements (and of L peaks in high-Z elements) is influenced by nearest-neighbor bonding. In other words, the chemical environment, on the atomic scale, can affect the x-rays produced by inner-shell ionizations, if the inner-shell electrons are influenced by nearest-neighbor interactions.

Figure 3-9 illustrates this phenomenon by showing the energy (wavelength) and shape of the carbon $K\alpha$ peak in different materials. Examination of this figure ought to convince you that not only is the peak shape dependent on the chemical environment, but so is the wavelength of the maximum intensity. This means, for example, that there exists no unique wavelength for $C_{K\alpha}$ x-rays corresponding to the maximum peak intensity. It would therefore be unwise to use the wavelength and intensity of $C_{K\alpha}$ x-rays determined on diamond to analyze carbon in graphite, or carbonates. We raise this issue for several reasons. First of all, you need to anticipate relatively

Figure 3-9 Variation in the area normalized peak shape and location for the carbon K line as measured from different

broad peaks in the low-energy range of the spectrum and choose the maximum intensity and background locations carefully. Secondly, you should be aware that although it is possible to analyze quantitatively for light elements, it is significantly more difficult to do so with the same accuracy as higher energy x-rays. This is due not only to the issues of peak shift and shape changes, which require quantitative calibration of relative peak and integral intensities, but also because of poorly determined corrections for absorption corrections and difficulties with high
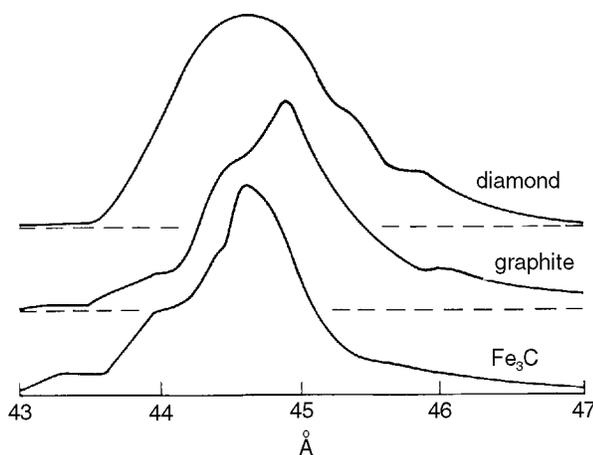
order interferences. So although it is possible to invest considerable time and effort in quantitative determinations of oxygen in silicates or carbon in carbonates, calculating them on the basis of stoichiometry or difference generally suffices. On the other hand, in many materials, the stoichiometric ratio of oxygen is variable or it appears as a trace contaminate. In these cases oxygen (or other light elements) should always be measured carefully for proper quantitative analysis.

Local bonding effects and peak shifts can be demonstrated especially well in metals versus oxides, and have been shown to be a problem in analyzing oxides with metal standards and vice versa (Sweatman & Long, 1969). This problem is generally remedied by choosing an appropriate standard (i.e., a standard as close as possible to the unknown). Aluminum, although not as severe an example as carbon is definitely influenced by the local chemical environment. The position and shape of the Al_{Ka} peak can differ depending on the coordination environment of Al (tetrahedral vs. octahedral). It is therefore prudent to select a standard for Al that has the same coordination as that expected in the unknown.

In some cases this non-characteristic behavior of peak position can be useful and indeed informative. Albee and Chodos (1971), for example have suggested that Fe^{++}/Fe^{+++} ratios can be semi-quantitatively determined with careful characterization of the L line x-rays, although their approach is now known to be flawed due to problems with self-absorption of the Fe $L\alpha$ x-rays. But if self-absorption for L edges is corrected for properly, this variation can be the basis for at least semi-quantitative determination of oxidation states.

3.2.6 X-ray absorption.

In order to detect (measure) an x-ray photon after it has been generated by an atom (and escapes from the atom) at some finite depth within the interaction volume, the x-ray must travel through the specimen and ultimately exit the surface. In order to fully understand and model the chemical composition of a sample with x–ray intensity data, it is therefore necessary to know how much of the initial x–ray intensity was absorbed between having been generated and finally exiting the specimen. Accounting for the absorption of x–rays is considered the primary correction to *raw* data, and can be as
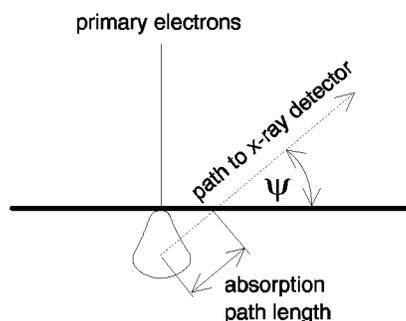

Figure 3-10 The path length for x-ray absorption from the interaction area through the sample line-of-sight to the detector. The angle between the planar surface and the line

high as 500% for a light element such as fluorine in a silicate mineral. The absorption correction for magnesium or aluminum can be as high as 25%, and for calcium or iron, on the order of 10%. Therefore, absorption by the specimen demands respect and understanding; absorption can be evaluated only if an accurate model for the x-ray generation volume is calculated. If the specimen is polished flat, the distance for absorption can be determined. As Figure 3-10 illustrates, the path

length an x-ray must follow through the specimen, and along which absorption can take place, involves knowing the *take-off angle*, Ψ.

The mathematical expression that accounts for the attenuation of radiation traveling through matter, as measured in the experiment depicted in figure 3-11, is known as Beer's law, where μ is known as the *linear absorption coefficient*. Beer's equation,

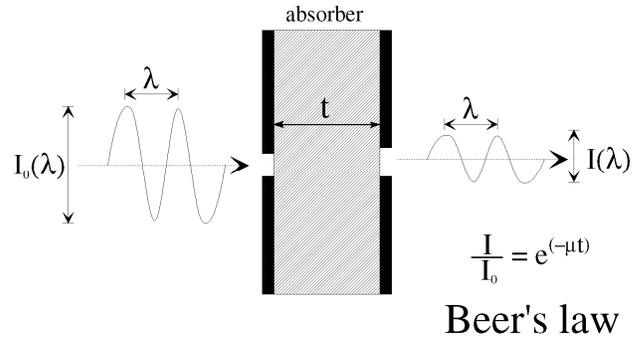$$\frac{I}{I_0} = e^{(-\mu t)}$$

eq. 3-6

Figure 3-11   Beer's law.

is the result of integrating a differential equation in which the absorption is proportional to the thickness of the absorber.

$$dI = (\mu I_0)\, dt$$

eq. 3-7

Notice that the experiment is set up to measure the intensity of the exiting radiation only at the initial wavelength (λ) and in the direction of the original radiation, i.e., changes in wavelength or direction are also defined as absorption. The attenuation measured is due to two types of processes, *true* absorption, μ_τ, and scattering, μ_σ, such that

$$\mu = \mu_\tau + \mu_\sigma$$

eq. 3-8

The two types of events that absorb x-rays are true or *photon* absorption, μ_t, and scattering. The latter is due to the interaction of the electromagnetic wave with the electrons of the atoms. The electrons are forced into oscillations by the absorbed x-ray and act as sources for scattered waves which can be of the same wavelength as the original wave (coherent or Rayleigh scattering), or of longer wavelengths, having given up energy (incoherent or Compton scattering). Coherent and incoherent scattering are a function of both the energy of the radiation and the binding energy of the electrons in the lattice, i.e., a resonance phenomenon. For our purposes, the scattering processes are insignificant for x-rays with wavelengths greater than 1Å (less than $\approx$12keV), and for absorbers of atomic number greater than 6. We will therefore focus our attention on true photon absorption.

We are primarily concerned with true or photon absorption not only because it is the primary mechanism for attenuating our x-ray signal, but also because ionization is the primary means by which an x–ray is absorbed within the specimen. When an x-ray is absorbed by photon absorption it generates a secondary x-ray from the atom doing the absorption. In other words, photon absorption results in the emission of another characteristic x–ray by fluorescence.   Figure 3-12 demonstrates the absorption of Fe Kα x-rays within a Fe-Cr alloy. Fe Kα x-rays (6.40keV) are sufficiently energetic to cause inner-shell ionization of the Cr atoms, thus producing Cr Kα x-rays. In this alloy, the intensity of Fe x-rays is decreased due to absorption whereas the intensity of Cr x-rays is enhanced.
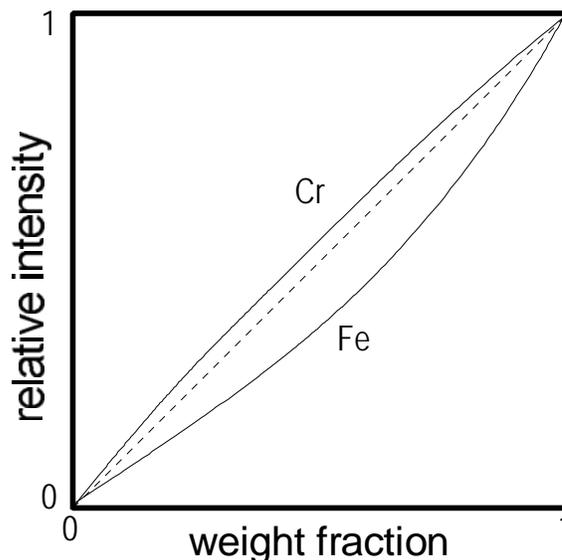

Figure 3-12   The fluorescence of Cr Kα x-rays due to absorption of Fe K.

The ability of atoms to attenuate emission of x-rays is almost independent of the chemical bonds and the structural arrangement of the phase in which those atoms are found. This is in contrast to the absorption spectra for less energetic radiation such as infrared and visible light that most definitely depends on bonds and structural features of the absorber. The basic reason for this difference is that most of the attenuation of x-rays involves inner-shell electrons of the absorber atoms, and these exist at energy levels that are not much affected by bonding and structure. Consequently, attenuation of x-rays of a given wavelength by atoms of a given type depends mostly on the number of atoms "seen" by an x-ray as it travels through the absorber.

Focusing our attention on photon absorption, corrections to raw counts as x-ray photons are emitted from the specimen will be a function of ionization of inner atomic shells by the characteristic x-ray radiation we are trying to measure. As defined above, the absorption coefficient is usually given with respect to a linear traverse through an absorber. This is known as a *linear absorption coefficient*. True absorption is the result of a finite number of "encounters", or events, along that path; the amount of absorption is therefore dependent on the density of the ionization sites. Since the linear density of atoms along any path in a phase is proportional to the bulk density of the phase, the parameter μ/ρ is a more generally useful one than just μ. The *mass absorption coefficient* *(μ/ρ)* depends on the chemical composition only and is independent of structural detail … which is to say, the μ/ρ for any of the polymorphs of sulphur is the same. Whereas the linear coefficient has dimensions of cm^{-1}, the mass coefficient has dimensions of cm^2/gram. Beers Law in terms of the mass absorption coefficient is:

$$\frac{I}{I_0} = e^{\left[\left(\frac{-\mu}{\rho}\right)(\rho t)\right]}$$

eq. 3-9

For a multi-element specimen, μ/ρ is the linear sum of the contributions from its individual elements, weighted according to mass concentration:

$$\mu_{mass}(\lambda) = \sum_i C_i \mu_{mass}(i, \lambda)$$

eq. 3-10

where μ_{mass} is the mass absorption coefficient μ/ρ and C_i is the weight fraction of the absorber. Since these are absorption coefficients normalized to mass, this mass averaging method is not only rigorously correct but also convenient for EPMA data recalculations. From this point on, in reference to absorption, we will refer to *mass absorption coefficients* only, for which its symbol will be simply μ rather than μ/ρ.

The mass absorption coefficient can be expressed by the following fit to experimental data:

$$\mu(a, \lambda) = \frac{N_{AV}}{A_a} \cdot c_{atomic} Z_a^4 \lambda^n = c \cdot \frac{Z_a^4}{A_a} \lambda^n \quad \propto \quad c' Z_a^3 \lambda^n$$

eq. 3-11

where *a* refers to some multi-element material; *n* ranges from 2.5 to 3.0 varying slightly with Z and λ; *c* and *c'* are constants which also vary a small amount with atomic number and wavelength. The approximation is due to the assumption that atomic weight varies smoothly with atomic number, which is neither true nor monotonic.

3.2.7 Absorption edges

Equation 3-11 implies a smooth increase in μ with both Z and λ. This turns out not to be the whole picture as demonstrated in Figure 3-13. The mass absorption coefficient plotted as a function of log wavelength should be a straight line with a slope *n*. Although the +4 slope is clearly present, superimposed on this trend are abrupt jumps or ***absorption edges***. The edges seen in Figure 3-13 are due to the presence of specific elements. An absorption edge for an element is the result of low absorption on one side due to the low probability of ionization with an x-ray with too little energy, and high absorption on the other side of the edge because the x-rays at that wavelength do have enough energy to be consumed by ionizing the absorber element. Figure 3-13 shows K line absorption edges for titanium and aluminum.
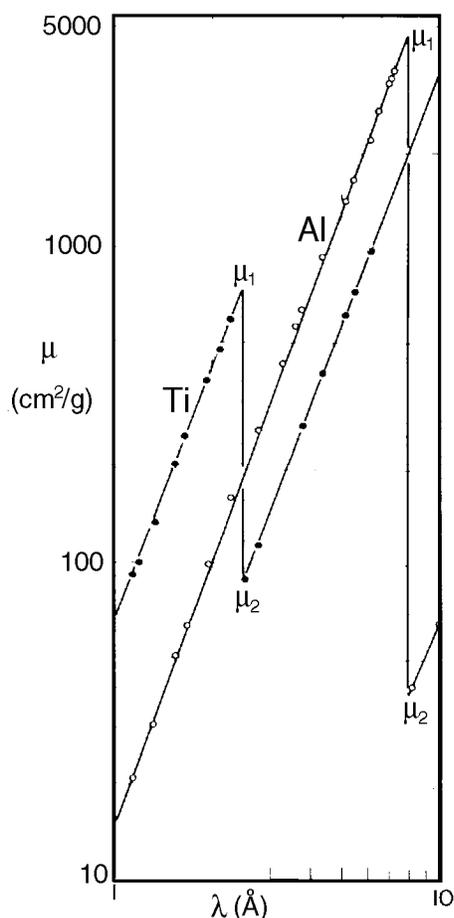
Figure 3-13 Mass absorption coefficients for aluminum and titanium. Both represent K shell ionization (from Heinrich, 1981).

Figure 3-14 Mass absorption for gold showing L and M shell ionization edges.

The line labeled "Ti" corresponds to absorption of different wavelengths of x-radiation in a Ti "target". The "points" on the line refer to the specific wavelengths of K lines for elements close to Ti in atomic number that are absorbed by Ti. Decreasing wavelength corresponds to increasing energy and increasing Z of the element producing that characteristic wavelength. Thus, the points on the line going away from the Ti-absorption edge toward lower wavelengths include V, Cr, Mn, Fe, Co, Ni and Cu, respectively. The wavelength for Ti_{Ka} corresponds to minimum point of the edge. Going away from the edge in the low energy direction, we encounter Sc, Ca, K, etc. The edge is due to the fact that x-rays with energies less (wavelengths greater) than that required to ionize the K-shell of Ti are not greatly absorbed (e.g., Ti, Sc, etc.) On the other hand, $V_{K\alpha}$ x-rays have sufficient energy to produce $Ti_{K\alpha}$ transitions, and therefore are strongly absorbed. Observations to note include the fact that μ/ρ increases with increasing Z of the absorber until the absorption edge effect; μ/ρ increases with λ until the absorption edge effect; Ti is relatively "transparent" to $Ti_{K\alpha}$ x-rays; Ti is relatively "opaque" to $V_{K\alpha}$ x-rays.

An absorption edge exists for each possible quantum transition. For the K-series, all of the possible transitions are so close in energy that they are indistinguishable in terms of absorption edges. High atomic number elements/absorbers, on the other hand typically exhibit multiple edges. Figure 3-14 shows the absorption edges for the L and M families of lines in gold.
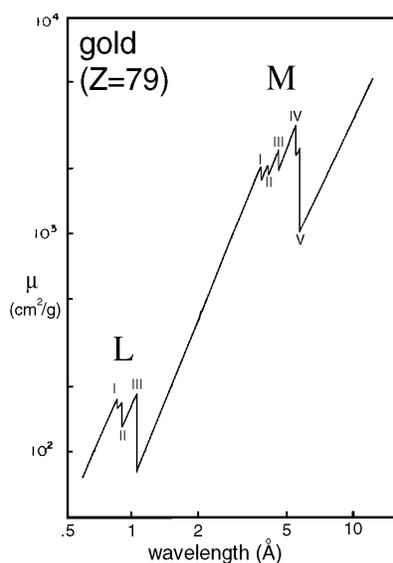
The important questions to ask with respect to absorption are: "How does absorption vary within different absorbers for a specific x-ray?", and "How does absorption vary for different x-ray wavelengths (with respect to Z) within a specific absorber?". Figure 3-15 addresses these questions by plotting both absorption for the $Si_{K\alpha}$ x-rays as they travel through varying atomic number absorbers, and the absorption of various x-rays by a silicon absorber. It differs from Figures 3-13 and 3-14 in that the abscissa is not logarithmic, and because wavelength decreases to the right with increasing Z. For the case of absorption of

$Si_{K\alpha}$ x-rays, note that absorption is relatively high in high-Z absorbers and that the absorption decreases with decreasing Z until the Si absorption edge. This steady decrease with decreasing Z is that predicted by equation 3-11. The absorption of $Si_{K\alpha}$ x-rays reaches its minimum value at the low-point of the Si absorption edge. Across the Si-absorption edge, the absorption of $Si_{K\alpha}$ x-rays increases by an order of magnitude and has a maximum value for the wavelength associated with the Al_{Ka} transition. Below the jump, absorption of $Si_{K\alpha}$ x-rays decreases again with Z as predicted by equation 3-11. In terms of other characteristic x-rays being absorbed by Si atoms, the trend is one of decreasing absorption with increasing Z. Very low-Z elements are strongly absorbed by Si atoms. The absorption decreases to a minimum value for Si Kα x-rays and then jumps up by an order of magnitude for P. Thereafter, absorption decreases steadily with increasing number.
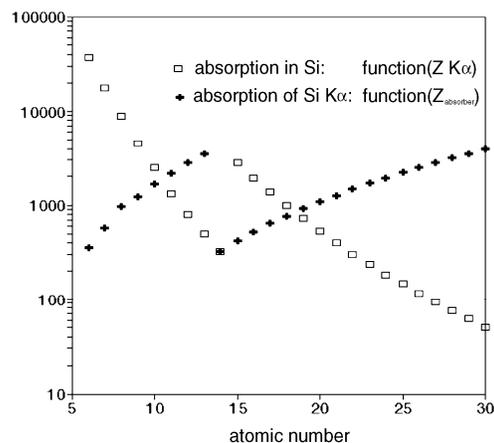

Figure 3-15 Absorption as function of atomic number for a specific x-ray wavelength and for a specific absorber.

Plots such as Figures 3-13, 3-14 & 3-15 illustrate the basic principles involving absorption. It is important to realize that absorption within a single-element target/absorber will be trivial (simply the value for μ in itself). It is only in multi-element specimens that absorption becomes interesting and more difficult to understand and model quantitatively. Each element present in the target will provide one or more absorption edges to the total absorption of the specimen. The degree to which each element's x-rays are absorbed by the multi-element specimen will primarily be dependent on the relationship of the energy of an element's characteristic x-rays to an absorption edge. A more realistic example of absorption effects is presented in Figure 3-16 which shows how various Kα x-rays are absorbed within our Kakanui Hornblende reference standard[4]. All Kα locations are shown for elements heavier than carbon and lighter than zinc. Each element present in this mineral (O, Na, Mg, Al, Si, K, Ca, Ti and Fe) provides at least one absorption edge (Fe provides two - the K-edge and an L-edge). All edges are for ionization of the K shells, except for iron, for which the edge due to L_{III} ionization is also shown. Notice the extreme range in mass absorption coefficients calculated for the x-rays of the elements we would want to analyze in a typical hornblende.

---

[4]   Figure 16 is a plot of calculated absorption values for all x-rays, $6 \leq Z \leq 30$, using Eq. 3-11. The data were taken from Heinrich, 1966. The absorption edges were plotted by location, for which vertical lines were extrapolated and drawn. Notice that the height of the edge is proportional the amount of the element present.
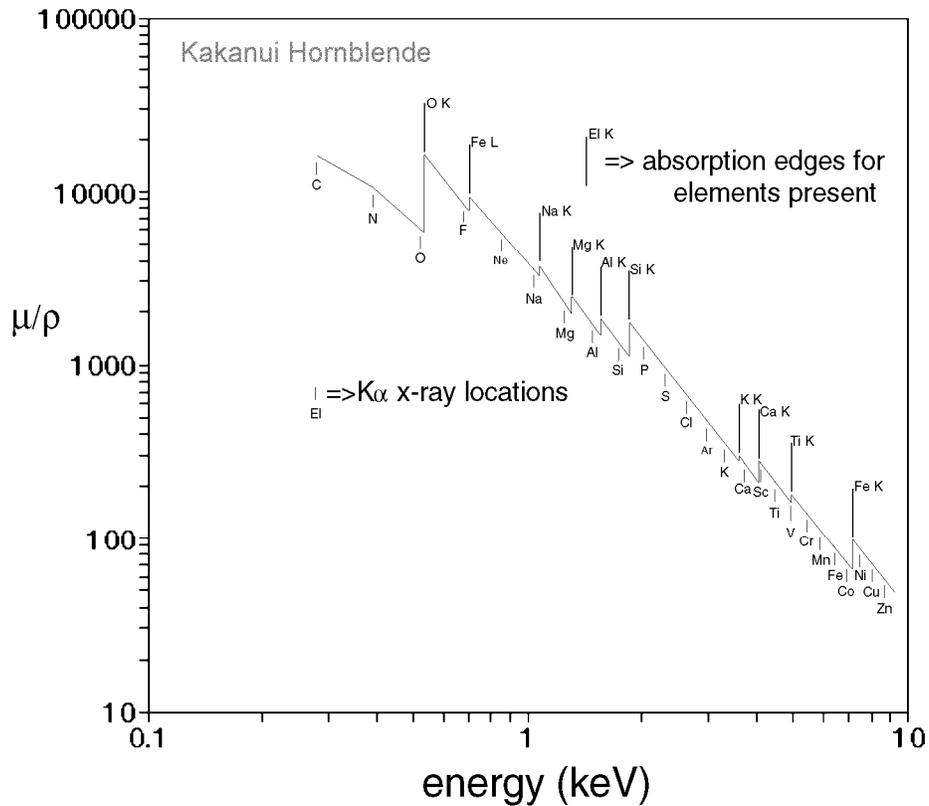
Figure 3-16   Absorption of various x-ray radiation for the Kakanui Hornblende reference standard. The edges indicate actually which elements are present, and the height of the edge being an approximate measure of the element's concentration.

In addition to equation 3-11, calculation of absorption coefficients for an x-ray within a multi-element absorber requires incorporation of the absorption edge effects. These effects include the location of the absorption edges within a particular specimen (be it a standard or an unknown) and the height of the absorption edge. The height of the edge is commonly referred to as the *absorption edge jump ratio*, which is defined as

$$r_{edge} = \frac{\mu_{max}}{\mu_{min}}$$

eq. 3-12

where μ_{max} and μ_{min} are the mass absorption coefficient values above and below the absorption edge, i.e., the high energy (low wavelength) and low energy (high wavelength) sides. Either the ratio or the difference between the two has been
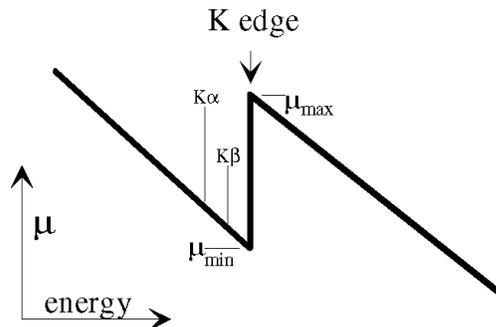

Figure 3-17   Absorption edge height and hypothetical K shell ionization (not to scale).

shown to vary smoothly as a function of atomic number for the pure elements. Therefore, its calculation and scaling with respect to the amount of the element present in a specimen can fairly easily be incorporated into a computer program for calculating x-ray intensities corrected for absorption.

Although Equation 3-11 combined with calculated jump ratios can be easily utilized with modern software to calculate absorption values, in practice, most x-ray correction programs utilize absorption data in the form of a "look-up table". The reason for this is because absorption is the most controversial, as well as the most significant, correction applied to x-ray intensities used for quantitative analysis. Indeed, the most commonly referenced compilation of absorption data is titled *X-Ray Absorption Uncertainty* (Heinrich, 1966)! Because of absorption uncertainties, most data reduction programs provide for the ability to change specific values or to use your own tables. A single computer algorithm doesn't provide for this versatility and flexibility. Our absorption coefficient and jump-ratio look-up table incorporates the latest "best values" (or at least the most accepted values), but they can be easily changed as new values are published in the literature.

The final points we wish to make regarding x-ray absorption edges are practical items of concern.   In the "bad old days" we used to have to calculate absorption corrections by hand, or rely on very crude computer programs. Nowadays, these calculations, although very rigorous are virtually "invisible" to the analyst. The "black box" character of a modern, computer-based instrument supposedly "takes care" of all of these absorption effects. We advise you, however, to accept the computer "corrections" with a healthy degree of skepticism. As noted above, absorption corrections, **especially near the absorption edges** are very uncertain. A good analyst will therefore be very careful when choosing an analytical line that lies very close to an edge (that is, when the ZAF correction is larger than 200%). Secondly, since the *bremsstrahlung* or background radiation is also subjected to absorption, background locations should also be chosen with similar care (i.e., never on the other side of the edge with respect to the analytical line of interest.

3.3 X-ray diffraction.

You are probably already familiar with *x-ray diffraction* because it is a very important analytical technique for crystal lattice determinations.   The technique you studied in your mineralogy or chemistry course uses characteristic x-ray radiation of a specific wavelength (e.g., Ni Kα) to determine crystal lattice dimensions and structure.   Having measured the lattice parameters, the x-ray diffraction analyst can determine the unknown mineral with a database listing of *d*-spacings.   Electron microprobe microanalysis uses x-ray diffraction in a different sense. All concepts remain the same, however in the case for EPMA, a known crystal *d*-spacing is used to measure an unknown x-ray wavelength, and is the primary means for x-ray spectrometry (WDS).

In terms of the wave concept applied to photons, x-rays are *specularly* reflected from a crystal's internal structure only if the elastically scattered (reflected) wave front of photons are in phase, i.e., do not destructively interfere with each other. This is the case for gratings as well as crystals only if parallel paths of incoming and reflected photons retain the phase relationship by

traveling path length differences equal to some multiple of the wavelength. For radiation of specific wavelengths (x-rays), specular radiation only occurs at a specific angle relative to the crystal's reflective layer, so termed the two-theta angle, 2θ, where theta is the entrance angle equal to the emergence angle.

The resultant relationship, as you are probably aware is *Bragg's law,*

$$n\lambda = 2d \, \sin\theta$$

<div align="right">eq. 3-13</div>

where *d* is the lattice spacing, and *n* is some integer. You might want to re-familiarize yourself with this relationship by reviewing a mineralogy or physics text. The most general derivation is given below, but presumes an existing understanding.

X-ray diffraction as applied to the determination of unknown minerals uses x-radiation from either nickel or copper, i.e., hard radiation. The point is, if known inorganic crystals are to be used for x-ray wavelength determinations, then the applicability is only for x-rays with short wavelengths. Because of the need for long wavelength determinations, *pseudo*-crystals with large *d*-spacings were developed. These materials are manufactured by attaching heavy atoms, e.g., lead, to large very molecules, e.g., sterates, and folding the sheet as many as a hundred times. Whereas these materials do have a *d*-spacing, unlike crystals they do not have any repeatable structure within the layer. Although introductory texts never implied any requirement for structure within the reflecting layer, you might still appreciate derivation for Bragg's law for the most general case. Referring to figure 3-18, for an incident wave front and emergent wave front from a material at depth spacing *d*, the path CB + BD must be equal to some multiple of the wavelength, in accordance with the phase relationship rule established earlier. In this most general case we are
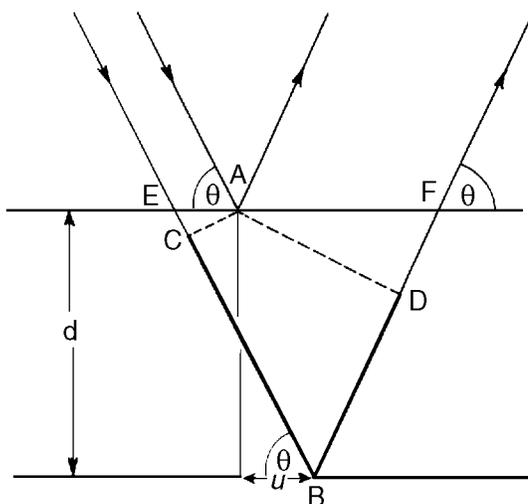

Figure 3-18   Illustrating Bragg's Law and the geometry for the most general case.

going to allow the point of scattering off the layer at depth to be some arbitrary horizontal distance, *u*, from that of the layer above, thereby removing dependence on placement of lateral scattering centers. From this we have

$$n\lambda \quad = CB + BD \quad = 2(EB) - EC - DF$$

$$if \quad EC \quad = EA\cos\theta \quad = (d\cot\theta - u)\cos\theta$$

$$and \quad DF \quad = FA\cos\theta \quad = (d\cot\theta + u)\cos\theta$$

$$n\lambda \quad = CB + BD \quad = 2d/\sin\theta - (d\cot\theta - u + d\cot\theta + u)\cos\theta$$

$$= 2d/\sin\theta - 2d\cot\theta\cos\theta$$

$$= 2d\sin^{-1}\theta(1 - \cos^2\theta)$$

$$= 2d\sin\theta$$

For precise measurement of x-rays, the Bragg equation needs to be corrected for the refractive index for x-rays in the crystal, σ_r

$$n\lambda \; = \; 2d\;\sin\theta\left(1 \; - \; \frac{(1 \; - \; \sigma_r)}{\sin^2\theta}\right)$$

<div align="right">eq. 3-14</div>

In the case for pseudo-crystals, and also in the more modern case of multi-layer dispersive elements (LDEs), the refractive index correction can become significant. However, many instruments incorporate such a factor when installing crystals for a spectrometer. The correction is usually of the form

$$n\lambda \; = \; 2d\;\sin\theta\left(1 \; - \; \frac{k}{n^2}\right)$$

<div align="right">eq. 3-15</div>

where the d-spacing and k-factor are known. For example, for the PET (pentaerythritol) crystal, d is 8.75Å and *k* is 0.000144.

An analyst who uses x-ray diffraction will need to anticipate the ramifications of *n*>1 when analyzing his or her spectrum which represents d-spacings for an unknown crystal. For example, for *n*=1, he/she would see a major peak for a specific d-spacing, and would need to anticipate the presence of another for *n*=2, for which there would be a peak indicative of half the real d-spacing.

As you might expect, there exist similar ramifications for the microprobe analyst. For example, if he/she were to scan the wavelength range of the crystal spectrometer; for *n*=1, the

spectra might show a peak indicative of an element, and other artifact peaks as well for $n=2, 3, ...$. This is not the usual use of the EPMA spectrometer, however. Elements are usually anticipated, to which the spectrometers are specifically tuned. Even for a spectrometer which is tuned to an $n=1$ x-ray wavelength another n>1 problem can exist. For example, consider the case for chromite (chromium-iron oxide). The Al Kα line has a wavelength of 8.340Å, and the Cr Kβ line, 2.085Å. The problem here is that when the crystal spectrometer is tuned to Al$_{K\alpha}$($n=1$), it is also tuned to Cr$_{K\beta}$($n=4$). And, of course, spectra locations for $n{\neq}1$ need be considered as possible interferences with background measurements.

3.4 Summary

Many of the concepts introduced in this chapter, and the previous, will be taken up again when we take a better look at quantifying the elements responsible for the x-ray emission. However, before we leave the subject of the nature of x-rays as they apply to EPMA, and discuss the instrument itself, you should insure you have a basic grasp of specimen interaction, x-ray generation and x-ray absorption. A good understanding will provide a good basis for analytical strategy.

For further general reading we might suggest Heinrich (1981) and Bertin (1971). Sweatman and Long (1969) is an excellent paper with specific regard to mineralogic specimens.